DOI 10.1007/s10517-020-05004-3

GENETICS

Abnormal Vasculature Development in Zebrafish Embryos with Reduced Expression of Pantothenate Kinase 2 Gene

D. Khatri[1], L. Mignani[1], D. Zizioli[1], M. Ritelli[2], E. Monti[1], and D. Finazzi[1]

Translated from *Byulleten' Eksperimental'noi Biologii i Meditsiny*, Vol. 170, No. 7, pp. 72-78, July, 2020
Original article submitted May 17, 2020

Mutations in *pank2* gene encoding pantothenate kinase 2 determine a pantothenate kinase-associated neurodegeneration, a rare disorder characterized by iron deposition in the globus pallidus. To extend our previous work, we performed microinjections of a new *pank2*-specific morpholino to zebrafish embryos and thoroughly analyzed vasculature development. Vessels development was severely perturbed in the head, trunk, and tail, where blood accumulation was remarkable and associated with dilation of the posterior cardinal vein. This phenotype was specific as confirmed by p53 expression analysis and injection of the same morpholino in *pank2*-mutant embryos. We can conclude that *pank2* gene is involved in vasculature development in zebrafish embryos. The comprehension of the underlining mechanisms could be of relevance for understanding of pantothenate kinase-associated neurodegeneration.

Key Words: *PANK2; zebrafish; coenzyme A; vasculature development*

Pantothenate kinase-associated neurodegeneration (PKAN), a rare autosomal recessive disorder characterized by the presence of iron deposits in the globus pallidus [5], is associated with mutations in *pank2* gene that encodes for the enzyme catalyzing the first step in coenzyme A (CoA) biosynthesis. It accounts for about 50% cases of neurodegeneration with brain iron accumulation disorders and can present with early onset, rapid progression and prevalence of extrapyramidal symptoms or with later onset, slower progression, parkinsonism, psychiatric and cognitive symptoms [4]. It is not clear yet, whether functional defects in *PANK*2 gene affect cellular CoA level [1,9]. Recent work suggests that defects in CoA homeostasis could lead to reduced 4'-phosphopantethenylation of mitochondrial acyl carrier protein and hence changes in lipoylation of several proteins, including pyruvate dehydrogenase [8]. Further studies are necessary to understand the biochemical and molecular pathways leading to PKAN. We recently contributed to this challenge by studying *pank2* in zebrafish embryos [6,14]. In zebrafish, *pank2* is mainly expressed in the CNS and in the vasculature. Knocking down *pank2* expression by a specific morpholino led to perturbations of the neuronal development and vasculature formation. We found impaired angiogenesis in mutant embryos with *PANK*2 overexpression [7] and with downregulation of the *coasy* gene [6], and also in mammalian cells with *PANK*2 silencing [10], which confirmed the relevance of CoA homeostasis for these processes. Vasculature function was not assessed in other animal models of PKAN.

Here, we describe the results of a more thorough analysis of the vasculature phenotype induced in zebrafish embryos by a different splice-inhibiting morpholino and conclude that the vasculature compartment is very sensitive to defects in *PANK*2 in zebrafish embryos.

[1]Section of Biotechnology, [2]Section of Biology and Genetics, Department of Molecular and Translational Medicine, University of Brescia, Brescia, Italy. ***Address for correspondence:*** daniela.zizioli@unibs.it. D. Zizioli

MATERIALS AND METHODS

Fish breeding, embryo collection, and treatments. Adult zebrafish and embryos were kept and analyzed as described previously [6,14]. Fish were used according to Directive 2010/63/EU of the European Parliament and of the Council (On the Protection of Animals used for Scientific Purposes; September 22, 2010). Adult zebrafish were maintained and used following the protocols approved by the Local Committee for Animal Health Protection (Organismo per il benessere animale). Generation of *pank2* mutant fish was approved by the Italian Ministry of Health (project 585/2018-PR).

Knock-down of *pank2* in zebrafish embryos. To knock-down *pank2* expression, wild-type embryos received microinjection of a specific morpholino (CTGTAGTGCAATAATAAGTAGGTGG, MO) (Gene Tools). A standard morpholino (CCTCTTACCTCAGTTACAATTTATA, STD) was injected as negative control. In most experiments, morpholino was injection in a dose of 1 pmol (8.5 ng) in 4 nl of 1× Danieau buffer (pH 7.6) into 1-cell stage embryos. After microinjection, the embryos were incubated in fish water supplemented with 0.003% phenylthiourea at 28°C to prevent pigmentation processes and were analyzed at 24 or 48 h post fertilization (hpf).

Generation of *pank2* mutant fish. We generated *pank2* mutant lines by the CRISPR/Cas9 technology. Single guide RNA (sgRNA) 5'-GGGGAAGTGCGCTCAGAGAGCGG-3' was generated according to the protocol described elsewhere [2]. *Cas9* mRNA was transcribed from pCS2-nls-zCas9 plasmid using mMessage Machine SP6 kit. Embryos were injected with a solution containing 340 ng/µl of Cas9 mRNA and 50 ng/µl of sgRNA. F0 founders were selected by DNA amplification (primers: F: 5'-GGGATGTACGGAGAAGCAGGAGG-3'; R: 5'-CCATGCCAAACCATGGGAAAGGC-3'), Heteroduplex Mobility Assay, and Sanger's sequencing. In the end, we obtained embryos carrying a homozygous 50-bp deletion in *pank2* gene (Δ50).

RNA extraction and real-time reverse transcription PCR (RT-PCR). Total RNA was extracted and amplified by real-time RT-PCR as described previously [14]. We calculated the relative levels of expression of the target genes by the ΔΔCT method as previously described [3].

Microscopy. The images of embryos were using an Axio Zoom.V16 stereo zoom microscope (Carl Zeiss) equipped with Axiocam 506 color digital camera with ZEN Pro software (Carl Zeiss). Fluorescence of transgenic lines was visualized using an illuminator HXP 200C (Carl Zeiss). For *in vivo* analyses, the embryos and larvae were anesthetized with 0.16 mg/ml tricaine and mounted in 1% low melting agarose gel. For the analysis of blood vessels development, we also used a high-end Lightsheet Z.1 microscope (Carl Zeiss). Images were captured by using the ZEN imaging software with the same magnification, laser intensity, and exposure. Processing and visualization of LSM (laser scanning microscopy) images were performed using arivis Vision 4D 2.12.2 software. To measure the diameter of the posterior cardinal vein (PCV) we analyzed embryos of each type using 2D visualization. In each image, PCV diameter was measured seven times at specific points corresponding to the origin of intersegmental vessels (ISV). Images were taken as a snap of arivis Vision 4D 3D reconstruction with the same orientation and magnification. For comparison of fluorescence intensity, all images were set with a minimum of 129 and a maximum of 6500 for the pixels/intensity histogram. Solid 3D reconstructions were generated using the isosurface setting of arivis Vision 4D, adjusting the threshold value for each image, in order to visualize all the fluorescent structures, regardless of their intensity.

Western blotting. Proteins were extracted by homogenizing 30 embryos in 200 mM Tris-HCl, 100 mM NaCl, 1 mM EDTA, 0.5% NP-40, 10% glycerol, 1 mM NaF, and 1 mM Na_3VO_4. The total protein extract (50 µg) was analyzed as described [14]. Images were acquired with LI-COR Odyssey image station, and band intensity quantified by ImageJ software without any modification of the original data.

Statistical analysis. We applied one-way ANOVA analysis with Tukey's correction for multiple comparisons or Student's *t* test to evaluate the significance of differences among groups with normally distributed values (Prism 6 software, GraphPad).

RESULTS

Analysis of the survival and Pank2 protein level in embryos injected with different doses of STD and MO at 48 hpf showed that the dose of 1 pmol was most effective in reducing Pank2 protein level with low embryo mortality (Fig. 1, *a*, *b*); hence it was selected for the study.

As Pank enzymes catalyze the first step in CoA biosynthesis, a decrease in Pank2 level could induce compensating changes in the expression of other *pank* and *coasy* genes. We compared the mRNA level of *pank1A* (P1a), *pank1B* (P1b), and *coasy* in morphants. While we did not find changes for *pank* isoforms, *coasy* mRNA was significantly augmented ($p<0.05$) (Fig. 1, *c*), indirectly confirming that *pank2* downregulation perturbs CoA biosynthesis.

We compared the morphology of morphants with wild-type (WT) and STD-injected embryos. While

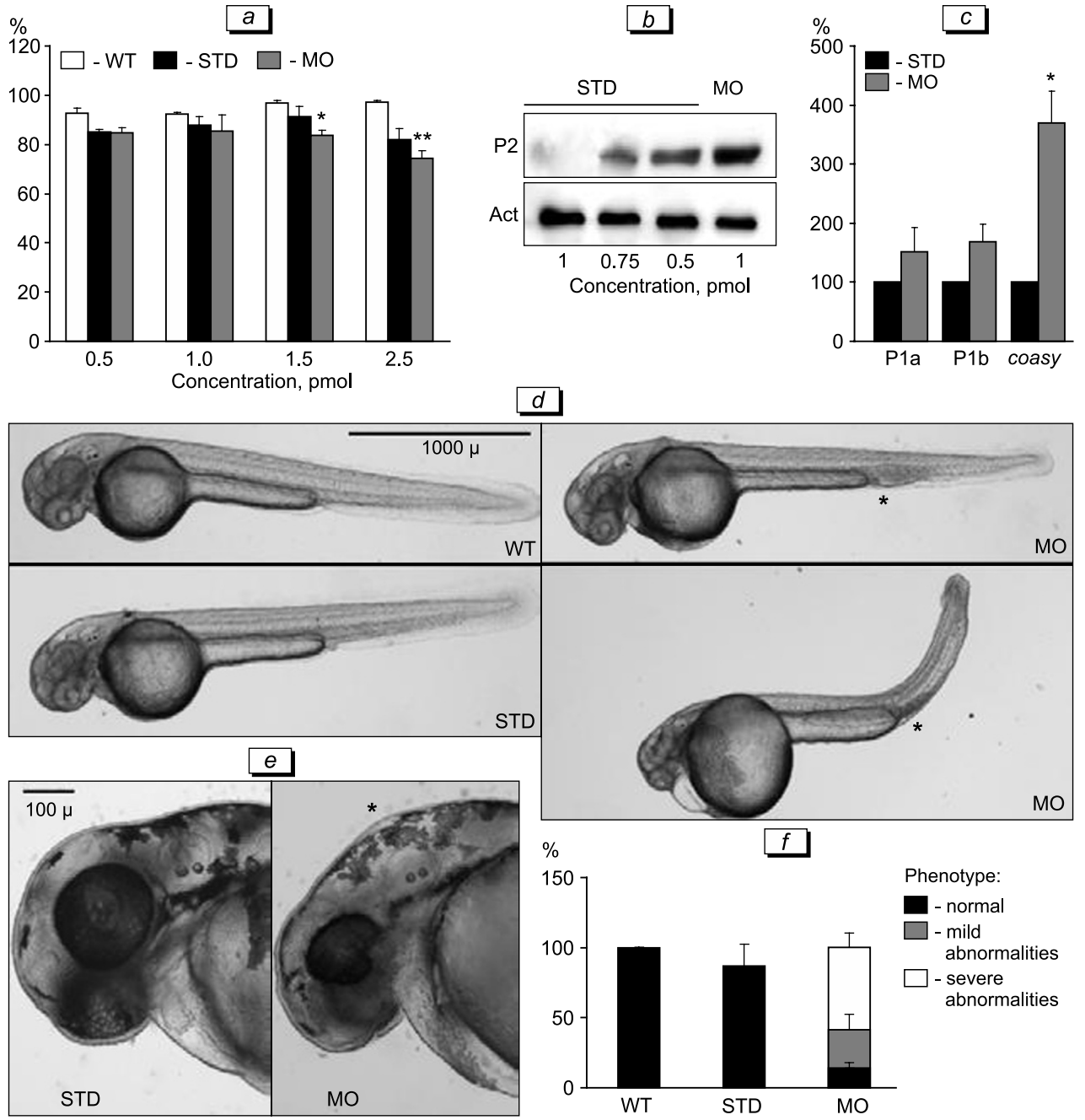

Fig. 1. Morphological analysis of MO-injected embryos at 48 hpf. *a*) Survival rate of embryos injected with different doses of STD or MO morpholinos; **p*<0.05 and ***p*<0.01. *b*) Representative Western blotting for PANK2 (P2) and actin (Act). *c*) real-time RT-PCR quantification of *pank* (P1a and P1b) and *coasy* mRNAs in MO-injected embryos (1 pmol) at 48 hpf. *d*) Lateral views of living anesthetized embryos at 48 hpf (for MO-injected embryos, representative images of mild and severe abnormalities are shown). *e*) Heads of STD- and MO-injected embryos. Asterisk points to hindbrain edema. *f*) Distribution of morphological phenotypes in MO-injected embryos.

more than 85% of STD-injected embryos had normal phenotype (170/194, *n*=5), most morphants (370/428, *n*=5) showed a perturbed morphology at 48 hpf (Fig. 1, *d-f*), with smaller head and edema at the hindbrain level (Fig. 1, *d*, *e*). The eyes were significantly smaller (STD 195.5±3.9 µ; MO 123.1±2.3 µ, $p<0.0001$). Blood accumulation in the trunk and the tail plexus were present (Fig. 1, *d*). Many morphants (248/428) showed a more severe phenotype with appearance of heart edema and curvature of the tail (Fig. 1, *d*).

We recently obtained fish carrying a homozygous deletion of 50 bp (Δ50) in exon 1 of *pank2* gene. The deletion should lead to a premature stop codon and abrogate the production of the full-length protein. The

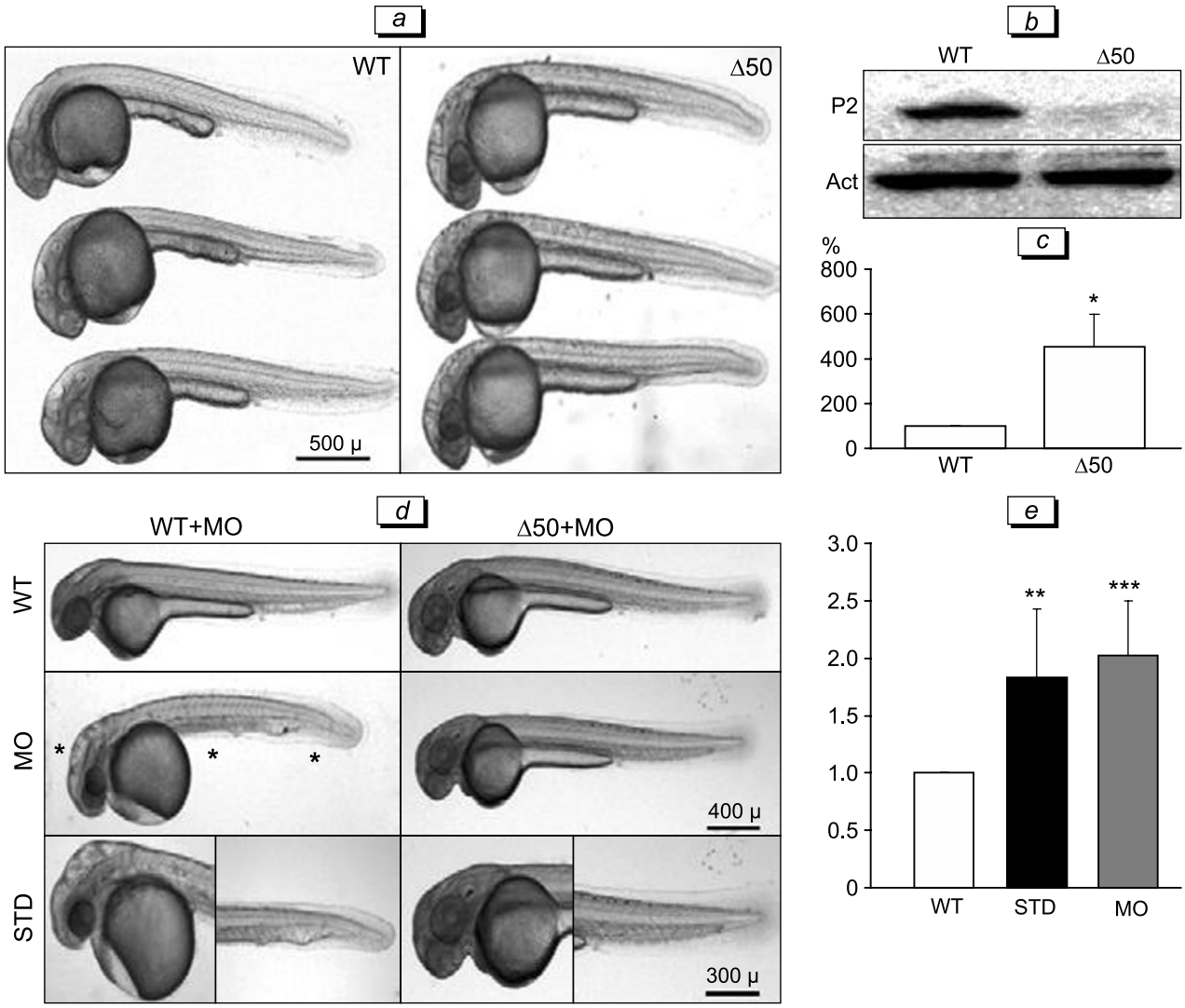

Fig. 2. Characterization of Δ50 mutant line and specificity controls for MO phenotype. *a*) Representative lateral views of wild-type (WT) and mutant Δ50 embryos at 48 hpf (150 embryos in 3 experiments). *b*) Immunoblotting analysis of PANK2 protein content wild-type (WT) and mutant Δ50 embryos at 48 hpf. *c*) qRT-PCR analysis of *coasy* mRNA in wild-type (WT) and mutant Δ50 embryos at 48 hpf (in 3 experiments) *$p<0.05$. *d*) Representative lateral views of wild-type (WT) and mutant (Δ50**)** embryos at 48 hpf after injection of MO (150 embryos in 2 experiments). Asterisks point to major morphological disturbances observed in all morphants. *e*) Analysis of *p53* mRNA levels in STD- and MO-injected embryos (in 3 experiments). **$p<0.01$, ***$p<0.001$ in comparison with WT embryos.

Western blotting analysis confirmed marked reduction of Pank2 protein content in mutant embryos at 48 hpf (Fig. 2, *b*). Embryos development appeared to be normal (Fig. 2, *a*) and no morphological alterations were evident. Interestingly, mutant embryos showed a significant increase in *coasy* (Fig. 2, *c*), but no changes in *pank* isoforms mRNA (not shown). The biochemical and behavioral features of the mutant line are still under study, we used it to check for possible off-target effects induced by microinjection of MO, as suggested by recent guidelines [13]. Mutant embryos injected with 1 pmol MO showed no morphological abnormalities (Fig. 2, *d*). On the contrary, the same dose induced the expected abnormalities when injected to WT embryos. This indicates the specificity of the phenotype observed in morphants. Further confirmation of the absence of off-target effects came also from the analysis of *p53* mRNA level (Fig 2, *e*), since no changes between embryos injected with STD and MO were revealed.

We took advantage of the Tg(*kdrl*:EGFP*;gata1a*:dsRED) transgenic line for detailed analysis of vascular endothelial cells and erythrocytes distribution. The vascular endothelial growth factor receptor *kdr-like* (*kdrl*) promoter drives green fluorescent protein expression in endothelial cells, while *gata1*a is a transcription factor required for hematopoiesis and is expressed in hematopoietic tissues. At 48 hpf,

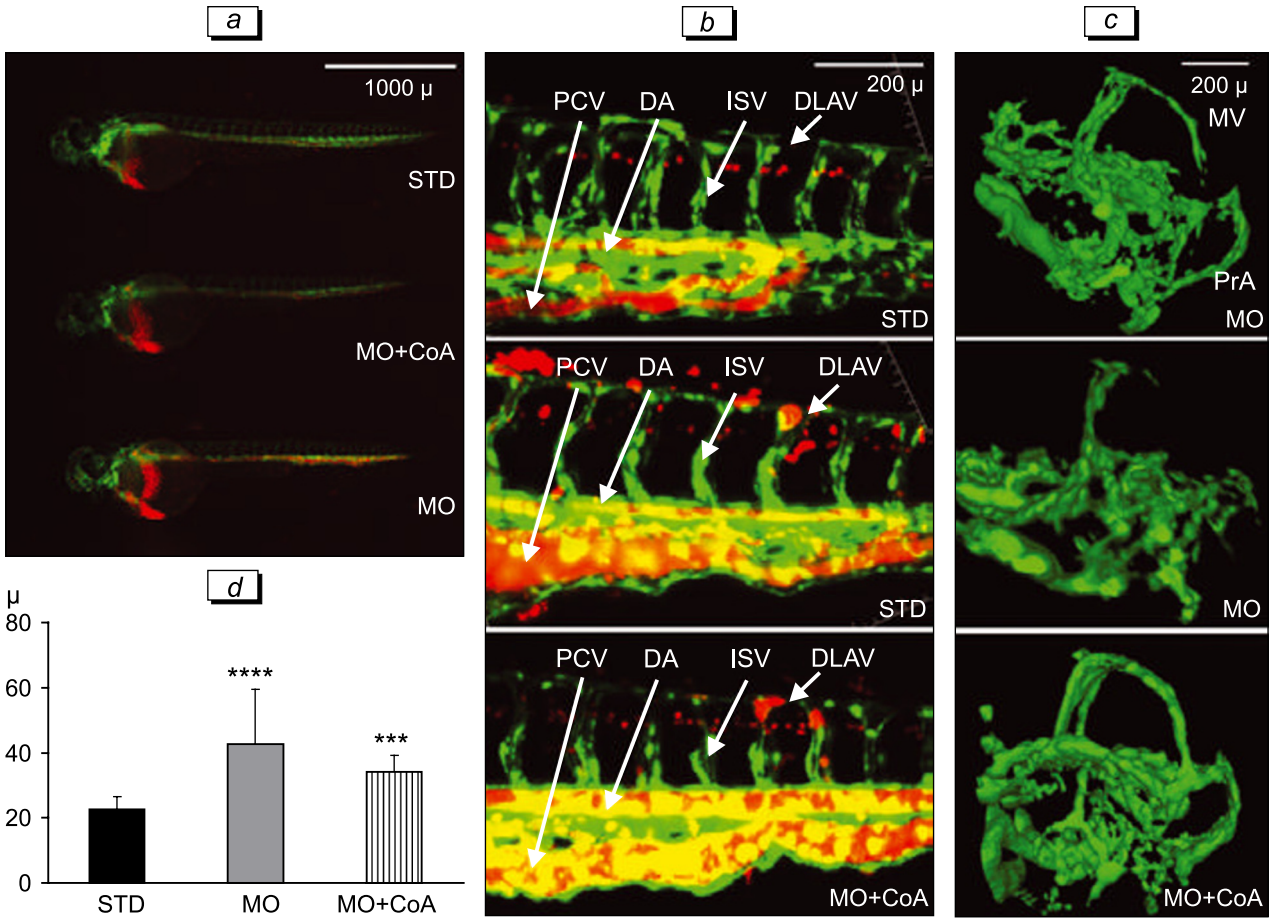

Fig. 3. Fluorescence analysis of Tg(*kdrl*:EGFP;*gata1*:dsRED) embryos injected with STD and MO morpholinos at 48 hpf. *a*) Lateral views of transgenic embryos injected with STD (*n*=167) or MO (*n*=164) morpholinos and eventually treated with 100 μM CoA (*n*=114) (in 3 experiments). *b*) Lateral views of the trunk section from STD- and MO-injected transgenic embryos at 48 hpf. LSM. DA, dorsal aorta; DLAV, dorsal longitudinal anastomotic vessel; ISV, intersegmental vessels; PCV, post cardinal vein. *c*) 3D reconstruction of head vessels in STD- and MO-injected embryos with and without CoA treatment (4 embryos of each type, in 3 experiments). MV, mesencephalic vein; PrA, prosencephalic artery. *d*) Changes in PCV diameter (*M*±*SD*). ***$p<0.001$, ****$p<0.0005$ in comparison with STD.

MO-injected embryos (160/164, *n*=4) showed a prominent accumulation of red blood cells at the caudal plexus and/or trunk (Fig. 3, *a*). In control embryos, dorsal aorta (DA), PCV, and ISV were already formed and contained circulating blood cells by 48 hpf, while in morphants, PCV was dilated and ISV were less regularly organized.

We analyzed this aspect in more details by LSM magnifying a section of the trunk from STD and MO-injected embryos with mild phenotype changes (Fig. 3, *b*; 5 embryos of each type, *n*=3); the analysis clearly confirmed the defects in the vascular structures, and in particular the dilation of PCV. The mean diameter of this vessel was enlarged in morphants in comparison with that in STD-injected embryos (Fig. 3, *d*). Then, we investigated vessels formation and distribution in the brain of morphants and control embryos at 48 hpf by LSM. When we imaged the head of the MO-injected embryo with the same parameters applied for the STD-injected one, we observed a decrease in EGFP fluorescence (not shown). This difference was evident when we built the solid 3D reconstruction of fluorescent structures (Fig. 3, *c*): the images clearly indicate the absence or poor development of some vascular structures, such as the mesencephalic vein and the prosencephalic artery in the MO-injected embryo.

It is known that defects in *pank2* gene can be corrected by addition of CoA [6,11,12]. The addition of 100 μM CoA to fish water of MO-injected embryos appeared to induce a better vascular development in MO-injected embryos, as also indicated by the reduction of PCV diameter (Fig. 3, *d*) and the improved arborization and development of head vasculature (Fig. 3, *c*). This work confirms the essential role of *pank2* in zebrafish vasculature development and may indicate a novel mechanism contributing to PKAN pathogenesis.

The work was supported by Health & Wealth Project (D. Finazzi) and ex60% funds from University

of Brescia (D. Zizioli and D. Finazzi). Dr D. Khatri (1st author) and Dr L. Mignani (2nd author) equally contributed to the work. L. Mignani is a student of the PhD program in Molecular Genetics, Biotechnology and Experimental Medicine from the University of Brescia, Italy.

D. Khatri and L. Mignani planned and performed the experiments, analyzed the data and corrected the manuscript, M. Ritelli and E. Monti analyzed the data and revised the manuscript, D. Zizioli and D. Finazzi conceived and planned the experiments, analyzed the data, prepared the figures, wrote and revised the manuscript.

REFERENCES

1. Di Meo I, Carecchio M, Tiranti V. Inborn Errors of Coenzyme A Metabolism and Neurodegeneration. J. Inherit. Metab. Dis. 2019;42(1):49-56. doi: 10.1002/jimd.12026
2. Gagnon JA, Valen E, Thyme SB, Huang P, Akhmetova L, Pauli A, Montague TG, Zimmerman S, Richter C, Schier AF. Efficient Mutagenesis by Cas9 Protein-Mediated Oligonucleotide Insertion and Large-Scale Assessment of Single-Guide RNAs. PLoS One. 2014;9(5):e98186. doi: 10.1371/journal.pone.0098186
3. Gatta LB, Vitali M, Verardi R, Arosio P, Finazzi D. Inhibition of heme synthesis alters Amyloid Precursor Protein processing. J. Neural. Transm. (Vienna). 2009;116(1):79-88. doi: 10.1007/s00702-008-0147-z
4. Gregory A, Polster BJ, Hayflick SJ. Clinical and genetic delineation of neurodegeneration with brain iron accumulation. J. Med. Genet. 2009;46(2):73-80. doi: 10.1136/jmg.2008.061929
5. Hayflick SJ, Westaway SK, Levinson B, Zhou B, Johnson MA, Ching KH, Gitschier J. Genetic, clinical, and radiographic delineation of Hallervorden-Spatz syndrome. N. Engl. J. Med. 2003;348(1):33-40. doi: 10.1056/NEJMoa020817
6. Khatri D, Zizioli D, Tiso N, Facchinello N, Vezzoli S, Gianoncelli A, Memo M, Monti E, Borsani G, Finazzi D. Down-regulation of Coasy, the Gene Associated With NBIA-VI, Reduces Bmp Signaling, Perturbs Dorso-Ventral Patterning and Alters Neuronal Development in Zebrafish. Sci. Rep. 2016;6:37660. doi: 10.1038/srep37660
7. Khatri D, Zizioli D, Trivedi A, Borsani G, Monti E, Finazzi D. Overexpression of Human Mutant PANK2 Proteins Affects Development and Motor Behavior of Zebrafish Embryos. Neuromolecular Med. 2019;21(2):120-131. doi: 10.1007/s12017-018-8508-8
8. Lambrechts RA, Schepers H, Yu Y, van der Zwaag M, Autio KJ, Vieira-Lara MA, Bakker BM, Tijssen MA, Hayflick SJ, Grzeschik NA, Sibon OC. CoA-dependent Activation of Mitochondrial Acyl Carrier Protein Links Four Neurodegenerative Diseases. EMBO Mol. Med. 2019;11(12):e10488. doi: 10.15252/emmm.201910488
9. Levi S, Finazzi D. Neurodegeneration with brain iron accumulation: update on pathogenic mechanisms. Front. Pharmacol. 2014;5:99. doi: 10.3389/fphar.2014.00099
10. Pagani F, Trivedi A, Khatri D, Zizioli D, Garrafa E, Mitola S, Finazzi D. Silencing of Pantothenate Kinase 2 Reduces Endothelial Cell Angiogenesis. Mol. Med. Rep. 2018;18(5):4739-4746. doi: 10.3892/mmr.2018.9480
11. Siudeja K, Srinivasan B, Xu L, Rana A, de Jong J, Nollen EA, Jackowski S, Sanford L, Hayflick S, Sibon OC. Impaired Coenzyme A Metabolism Affects Histone and Tubulin Acetylation in Drosophila and Human Cell Models of Pantothenate Kinase Associated Neurodegeneration. EMBO Mol. Med. 2011;3(12):755-766. doi: 10.1002/emmm.201100180
12. Srinivasan B, Baratashvili M, van der Zwaag M, Kanon B, Colombelli C, Lambrechts RA, Schaap O, Nollen EA, Podgoršek A, Kosec G, Petković H, Hayflick S, Tiranti V, Reijngoud DJ, Grzeschik NA, Sibon OC. Extracellular 4'-phosphopantetheine Is a Source for Intracellular Coenzyme A Synthesis. Nat. Chem. Biol. 2015;11(10):784-92. doi: 10.1038/nchembio.1906
13. Stainier DYR, Raz E, Lawson ND, Ekker SC, Burdine RD, Eisen JS, Ingham PW, Schulte-Merker S, Yelon D, Weinstein BM, Mullins MC, Wilson SW, Ramakrishnan L, Amacher SL, Neuhauss SCF, Meng A, Mochizuki N, Panula P, Moens CB. Guidelines for morpholino use in zebrafish. PLoS Genet. 2017;13(10):e1007000. doi: 10.1371/journal.pgen.1007000
14. Zizioli D, Tiso N, Guglielmi A, Saraceno C, Busolin G, Giuliani R, Khatri D, Monti E, Borsani G, Argenton F, Finazzi D. Knock-down of Pantothenate Kinase 2 Severely Affects the Development of the Nervous and Vascular System in Zebrafish, Providing New Insights Into PKAN Disease. Neurobiol. Dis. 2016;85:35-48. doi: 10.1016/j.nbd.2015.10.010